

## NEUTRON DIFFRACTION INVESTIGATION OF THE ANTIFERROMAGNETISM OF THE CARBONATES OF MANGANESE AND IRON

R. A. ALIKHANOV

Institute of Physics Problems, Academy of Sciences, U.S.S.R.

Submitted to JETP editor February 11, 1959

J. Exptl. Theoret. Phys. (U.S.S.R.) **36**, 1690-1696 (June, 1959)

A procedure is developed for low-temperature powder neutron diffraction. The antiferromagnetic structure of  $\text{MnCO}_3$  and  $\text{FeCO}_3$  is investigated. It is shown that in the antiferromagnetic state the spins in  $\text{MnCO}_3$  lie in the basis plane and in the symmetry plane. In  $\text{FeCO}_3$  the spins are directed along the rhombohedral axis. According to Dzyaloshinskiĭ, this means that  $\text{MnCO}_3$  is weakly ferromagnetic and  $\text{FeCO}_3$  is not.

INTEREST in isomorphous carbonates has been raised in connection with the investigations of the magnetic susceptibility of polycrystalline  $\text{MnCO}_3$  and  $\text{CoCO}_3$ , carried out by Borovik-Romanov and Orlova,<sup>1</sup> and the theory of the weak antiferromagnetic ferromagnetism observed in these substances, developed by Dzyaloshinskiĭ.<sup>2</sup>

Dzyaloshinskiĭ has analyzed the magnetic symmetry of the crystals and established a connection between the occurrence of weak ferromagnetism and the symmetry of the crystal. For the carbonates of manganese, iron, and cobalt, which crystallize in a rhombohedral system, three types of magnetic symmetry are possible: 1) spins directed along the rhombohedral axis, 2) spins lying in the basis plane and directed along the two-fold axis, 3) spins lying in the basis plane and in the symmetry plane.

There is no weak ferromagnetism in the first case, but it should be observed in the two remaining cases.

Neutron-diffraction procedures, unlike other methods of investigation of magnetism, make it possible to determine directly which of the magnetic structures occurs in a given crystal.

### EXPERIMENT

Crystalline carbonates of manganese and iron are difficult to obtain; therefore these substances were investigated by the powder method in a monochromatic neutron beam.

To obtain a monochromatic beam, a white neutron beam from the reactor\* was aimed at a lead

single crystal (see Appendix). The monoenergetic neutrons with  $\lambda = 1.37 \text{ \AA}$ , reflected at a given angle, were scattered by a polycrystalline specimen, placed in a low-temperature cryostat. The latter was the metallic hydrogen-filled Dewar of Kapitza,<sup>4</sup> in which thin-wall cylindrical aluminum shells, surrounding the specimen, were hermetically connected to the lower portions of the vacuum jacket and of the nitrogen shield. The specimen was placed in an inner aluminum cup, the upper end of which was soldered directly to the vessel with the cooling agent, and the bottom of which was fastened to a carbon resistor\* for measuring the temperature.

The instrument, first evacuated to  $2 \times 10^{-5}$  mm mercury, maintained the specimen at helium temperature for two days. The total amount of helium necessary for this purpose, including the cooling of the instrument, amounted to 7.5 liters.

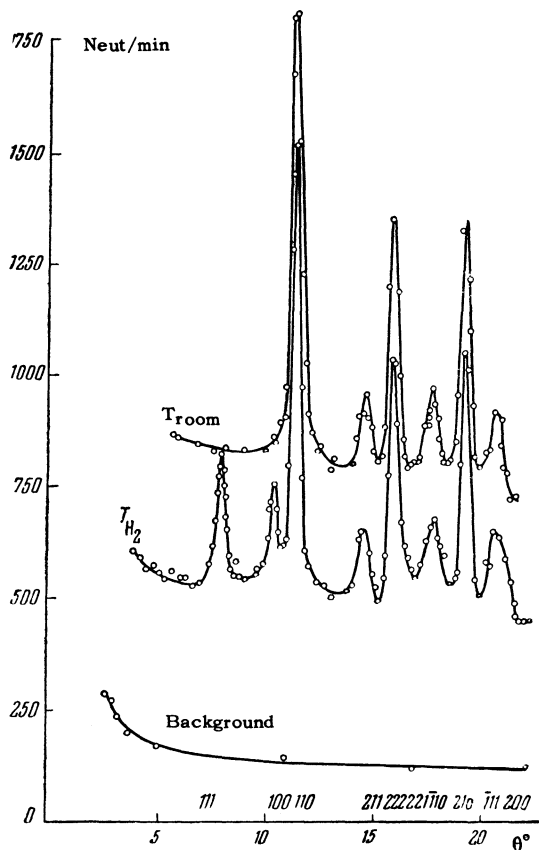
The neutron-scattering pattern was registered with a spectrometer constructed by Abov<sup>5</sup> and adapted for operation with a monochromatic beam.

### RESULTS AND THEIR DISCUSSION

**$\text{MnCO}_3$ .** Neutron diffraction patterns of  $\text{MnCO}_3$ , obtained with  $\text{MnCO}_3$  powder at room and hydrogen temperatures, are shown in Fig. 1. As can be seen from this diagram, the diffraction pattern changes as the temperature is decreased. At hydrogen temperature, in addition to a reduction in the diffuse thermal scattering, new reflections are produced at small Bragg angles. Figure 1 shows the reflection indices calculated from the relation for a quadratic form of rhombohedral subsyngony. The lat-

\*The work was carried out in the heavy-water reactor of the Institute of Theoretical and Experimental Physics, Academy of Sciences, U.S.S.R.<sup>3</sup>

\*We express our gratitude to Yu. V. Sharvin for supplying us with an experimental model of the thermometer.

FIG. 1. Neutron diffraction patterns of  $\text{MnCO}_3$ .

tice constants used were<sup>6</sup>  $a = 5.84 \text{ \AA}$  and  $\alpha = 47^\circ 15'$ . To verify the overall pattern of nuclear reflections, and for indexing purposes, we calculated the relative intensities of the nuclear peaks.

The coherent-scattering intensity  $P$  is given by<sup>7</sup>

$$\frac{P}{I_0} = \frac{B_j F^2 e^{-2W} A_{hkl}}{\sin \theta \sin 2\theta},$$

where  $I_0$  is the number of incident-beam neutrons per minute per square centimeter,  $B$  a constant for the given experiment,  $A_{hkl}$  the absorption factor,  $e^{-2W}$  the thermal coefficient,  $j$  the number of equivalent planes, and  $F$  the structure factor. The last two quantities vary with scattering angle. The absorption factor  $A_{hkl}$  depends in a complicated manner on the coefficient of linear absorption and on the radius of the specimen, which are constant for any given experiment. The thermal coefficient is connected with the characteristic temperature of the substance. The dependence of  $A_{hkl}$  and  $e^{-2W}$  on  $\theta$  is very weak and remains practically unchanged for the angle interval under consideration.<sup>7</sup>

Thus, to calculate the relative intensity of nuclear reflections it is necessary to calculate the structure factor. In the general form, the nuclear structure factor is written

$$F_{\text{nuc}} = \sum b \exp \{2\pi i (hx/a_0 + ky/b_0 + lz/c_0)\},$$

where  $b$  is the amplitude of nuclear scattering. According to the data gathered in reference 7,

$$b_{\text{Mn}} = -0,37 \cdot 10^{-12} \text{ cm}, \quad b_{\text{O}} = 0,58 \cdot 10^{-12} \text{ cm}, \\ b_{\text{C}} = 0,66 \cdot 10^{-12} \text{ cm}$$

respectively for manganese, oxygen, and carbon;  $x$ ,  $y$ , and  $z$  are the nuclear coordinates given in reference 6, while  $a_0$ ,  $b_0$ , and  $c_0$  are the dimensions of the elementary crystallographic cell, in this case equal to each other.

After inserting the coordinates of the atoms and after making several transformations, the square of the structural factor for even and odd sums of the Miller indices can be written in the following manner

$$1) \quad h + k + l = 2n + 1 \quad (n = 0, 1, 2, \dots):$$

$$F_{hkl}^2 = 4b_{\text{O}}^2 [\sin \{2\pi \cdot 0,27 (h - k)\} + \sin \{2\pi \cdot 0,27 (l - h)\} \\ + \sin \{2\pi \cdot 0,27 (k - l)\}]^2. \quad (1)$$

$$2) \quad h + k + l = 2n:$$

$$a) \quad (h + k + l)/2 = 2n:$$

$$F_{hkl}^2 = 4 \{b_{\text{C}} + b_{\text{Mn}} + b_{\text{O}} [\cos \{2\pi \cdot 0,27 (h - k)\} \\ + \cos \{2\pi \cdot 0,27 (l - h)\} + \cos \{2\pi \cdot 0,27 (k - l)\}]\}^2. \quad (2)$$

$$b) \quad (h + k + l)/2 = 2n + 1,$$

$$F_{hkl}^2 = 4 \{b_{\text{C}} - b_{\text{Mn}} + b_{\text{O}} [\cos \{2\pi \cdot 0,27 (h - k)\} \\ + \cos \{2\pi \cdot 0,27 (l - h)\} + \cos \{2\pi \cdot 0,27 (k - l)\}]\}^2. \quad (3)$$

The calculated intensities are listed in Table I, with accuracy to within a constant factor as compared with the observed intensity at hydrogen temperature. The constant factor is obtained by comparison with the two most intense reflections (110), (222).

TABLE I

Index	$\theta$		$i$	Relative intensity	
	calculated	observed		calculated	observed
111	$7^\circ 45'$	$7^\circ 54'$	1	0	350
100	$9^\circ 59'$	$10^\circ 7'$	2	0	290
110	$11^\circ 13'$	$11^\circ 13'$	6	1040	1050
211	$14^\circ 25'$	$14^\circ 25'$	6	165	200
222	$15^\circ 38'$	$15^\circ 40'$	2	690	670
221	$16^\circ 27'$	—	6	0	background
$\bar{1}10$	$17^\circ 23'$	$17^\circ 30'$	3	36	220
210	$19^\circ 9'$	$18^\circ 59'$	12	625	690
$\bar{1}\bar{1}\bar{1}$	$20^\circ 21'$	—	6	0	background
200	$20^\circ 53'$	$20^\circ 27'$	6	65	200

An important result is the forbiddenness of nuclear reflections (111) and (100), which follow from formula (1). As can be seen from Fig. 1, these reflections are actually missing at room temperature. However, they do arise as the temperature is reduced to that of hydrogen. It is natural to assume that they are due to magnetic ordering. For the same reason, an increase is seen in the intensity of nuclear reflections ( $\bar{1}10$ ), (210), (200), which are neighbors to the magnetic reflections (221) and ( $\bar{1}\bar{1}1$ ). Certain discrepancies between the compared values for the reflection (211) may be due to insufficient purity of the specimen.

Analysis of magnetic reflections. As shown by Halpern and Johnson,<sup>8</sup> the square of the summary structure factor in both nuclear and magnetic coherent reflection, for unpolarized neutrons, is

$$F^2 = F_{\text{nuc}}^2 + q^2 F_{\text{m}}^2$$

where  $q$  is the sine of the angle between the magnetization and scattering vectors.

For rhombohedral  $\text{MnCO}_3$  and  $\text{FeCO}_3$ , in the case of purely antiferromagnetic spin distribution in the elementary cell, the magnetic portion of the square of the structural factor can be represented as

$$q^2 F_{\text{m}}^2 = p^2 \sin^2 \beta |1 - e^{\pi i(h+k+l)}|^2, \quad (4)$$

where  $p = (e^2 \gamma / mc^2) S f$  is the magnetic scattering amplitude. The ion form factor  $f$  depends on the scattering angle.

When  $h + k + l = 2n$ ,  $n = 0, 1, 2, \dots$ , we have

$$q^2 F_{\text{m}}^2 = 0. \quad (5)$$

It follows from this that reflections with an even number of indices have no magnetic component. For  $h + k + l = 2n + 1$

$$q^2 F_{\text{m}}^2 = 4 (e^2 \gamma / mc^2)^2 S^2 f^2 \sin^2 \beta. \quad (6)$$

Thus, the scattering picture in the presence of antiferromagnetic ordering should contain, for a given lattice, only magnetic reflections with an odd index sum. However, even in this case  $q^2 F_{\text{m}}^2$  may vanish if the scattering vector is aligned with the magnetization vector. Such a case is possible in scattering from the (111) plane and antiferromagnetic arrangement of the spins along the rhombohedral axis.

The new reflections on the neutron-diffraction pattern for  $\text{MnCO}_3$  which occur at hydrogen temperature, are induced precisely by the indices with odd sum (111) and (100). Those following — (221), (210) and ( $\bar{1}\bar{1}1$ ) — are not resolved because of the low intensity. Their presence makes itself felt in a certain change in the bases of the

nuclear peaks (222), ( $\bar{1}10$ ), and (200) and in an increase in the intensity of (210).

Since the reflection (111) is present in  $\text{MnCO}_3$ , the first of the three possible antiferromagnetic spin orientation, mentioned at the beginning of this article, namely along the rhombohedral axis, drops out. To choose between the two remaining orientations, it is necessary to compare, in both cases, the calculated and observed ratios of reflection intensities  $P_{(100)}/P_{(111)}$ . In accordance with the formula for the intensity, this ratio is

$$\frac{P_{(100)}}{P_{(111)}} = \frac{j_{(100)}}{j_{(111)}} \frac{\sin \theta_{(111)}}{\sin \theta_{(100)}} \frac{\sin 2\theta_{(111)}}{\sin 2\theta_{(100)}} \frac{f_{(100)}^2 \cos^2 \rho_{(100)}}{f_{(111)}^2 \cos^2 \rho_{(111)}}, \quad (7)$$

where  $\rho$  is the angle between the spin directions [uvw] and the plane (hkl) ( $\rho = \pi/2 - \beta$ ).

The experimental ratio of the intensities of magnetic reflections is  $P_{(100)}/P_{(111)} = 0.82$  (in the calculations we used the data of Shull, Strauser, and Wollan<sup>9</sup> for the form factor of  $\text{Mn}^{++}$ ). On the other hand, the expected values for the spins along the two-fold axis or in the symmetry plane are 1.29 and 0.81 respectively. Thus, the antiferromagnetic spins in  $\text{MnCO}_3$  lie in the symmetry plane normal to the three-fold axis.

**FeCO<sub>3</sub>.** The structure of  $\text{FeCO}_3$  was studied with a specimen of siderite from the Bokal (U.S.S.R.) deposit. Figure 2 shows the neutron diffraction pattern, taken at hydrogen temperature. The amplitude of nuclear scattering of  $\text{Fe}^{++}$  is more than double that of  $\text{Mn}^{++}$ , so that it became possible to record the neutron-scattering pattern with an automatic recording instrument. Table II lists the calculated and measured relative intensities for the first group of peaks.

As in the case of  $\text{MnCO}_3$ , the appearance of the (100) reflection at hydrogen temperature is evidence of the establishment of an antiferromagnetic structure. The absence of the (111) reflection, in accordance with the foregoing, means that the spins in  $\text{FeCO}_3$  are directed along the rhombohedral axis. This result confirms the conclusions of Bizette<sup>11</sup> concerning the antiferromagnetic structure of iron carbonate. It is interesting to follow also the temperature dependence of the magnetic reflection (100). Figure 3 shows this dependence, plotted as the instrument was heated after evaporation of the hydrogen. As follows from the graph, this specimen of  $\text{FeCO}_3$  goes into the antiferromagnetic state in the region of 35° K.

I express my deep gratitude to Academician P. L. Kapitza for continuous interest in the work, and also to A. S. Borovik-Romanov for useful advice. I also thank I. E. Dzyaloshinskiĭ for valuable discussion and Yu. G. Abov, for much useful coun-

FIG. 2. Neutron diffraction pattern of FeCO<sub>3</sub> at liquid-hydrogen temperature.

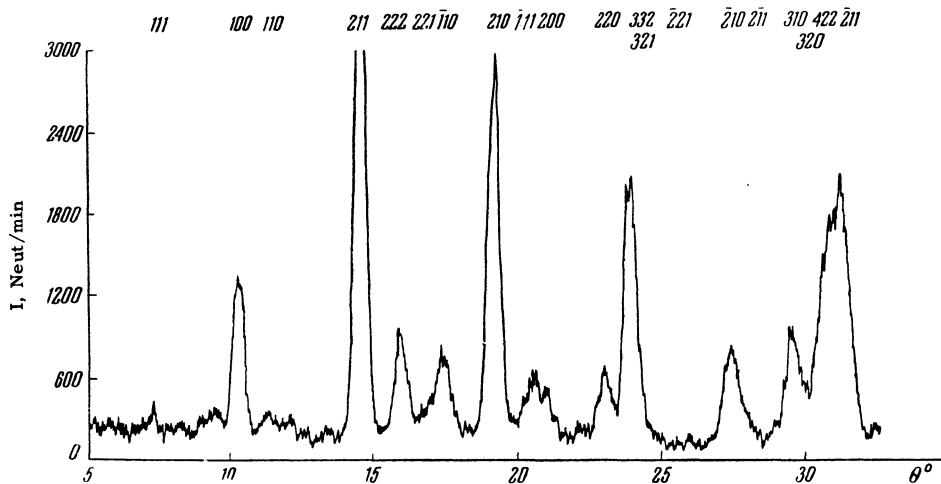


TABLE II

Index	Relative intensity		Index	Relative intensity	
	calculated	observed		calculated	observed
111	0	back-ground	222	110	117
100	0	150	110	117	90
110	5,7	back-ground	210	375	450
211	810	800	111	0	80
			200	66	70

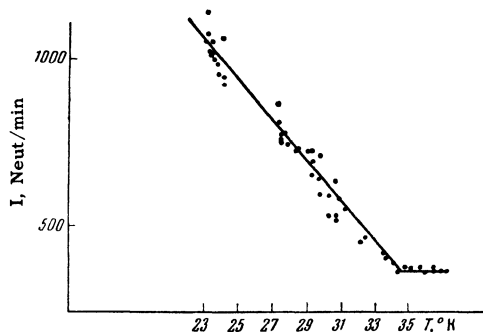


FIG. 3. Temperature dependence of magnetic reflection for FeCO<sub>3</sub> (from the Bakal deposit).

sel on the neutronoscopic portion of the investigation.

APPENDIX

1. The crystal area necessary to obtain a monochromatic beam amounts to 100 cm<sup>2</sup>. In connection with this, we constructed a special setup to grow, by the Kapitza method,<sup>10</sup> crystals of large area with specified orientation. When successfully grown, the crystal is obtained directly in final form and serves as a monochromator.\* The

\*The author expresses his gratitude to N. N. Mikhaïlov for his continuous assistance in growing crystals.

apparatus for growing is arranged as follows (see Fig. 4). A form, 2, of required size was flanged on an aluminum support plate, 1. The form is filled with lead. A glass dome attached to cover 4 permits evacuation of the volume and protects the lead against oxidation during growing, and also affords a certain reduction in heat loss.

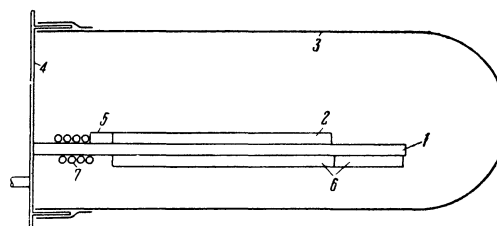


FIG. 4

Located in the narrow channel 5 of the forward cold portion of the mold is a primer, slightly buoyed up by the slowly advancing liquid phase of the lead. The boundary of two phases — the solid and the liquid — moves towards the cold portion which is heated by the small furnaces 6. At the instant when the primer starts floating, the temperature gradient increases rapidly as a result of the passage of compressed air through the cooling coil 7. Dependable single-crystal growth was attained after selecting: a) the shape of the cold portion of the mold, b) the growth rate, and c) the magnitude of the sliding temperature gradient.

The cold portion in final form resembles most closely the projection of a bird's head on a horizontal plane. The growing time did not exceed ten minutes, and the temperature gradient was 200° over the entire length of the crystal (16 cm).

For most effective reflection of the neutrons it is necessary to use the crystal plane with the maximum of atoms. This was the (111) plane, which, when placed in the plane of the plate or close to it,

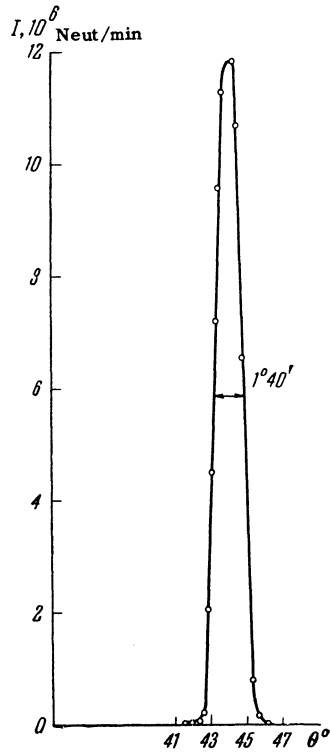


FIG. 5

could be observed during the time of growth by its characteristic light reflection, close to specular. Thus it became possible to control the growing process during the very growth of the crystal.

2. X-ray analysis of the crystals was made by plotting "epigrams." The reflection spots on the epigrams had a unique structure, indicating a considerable mosaic structure in the resultant crystals.

3. Using one such single-crystal plate we obtained a monochromatic beam of neutrons, the reflection curve of which is shown in Fig. 5. The intensity of the beam can be increased above  $12 \times 10^6$  per minute by greatly narrowing the beam.

An analysis of the monochromatic beam for higher-order reflections is shown in Fig. 6. Worthy of attention is the considerable intensity of reflection (222). The admixture of second-order reflections does not exceed 0.1%.

The properties of grown single crystals will be considered in greater detail in the future.

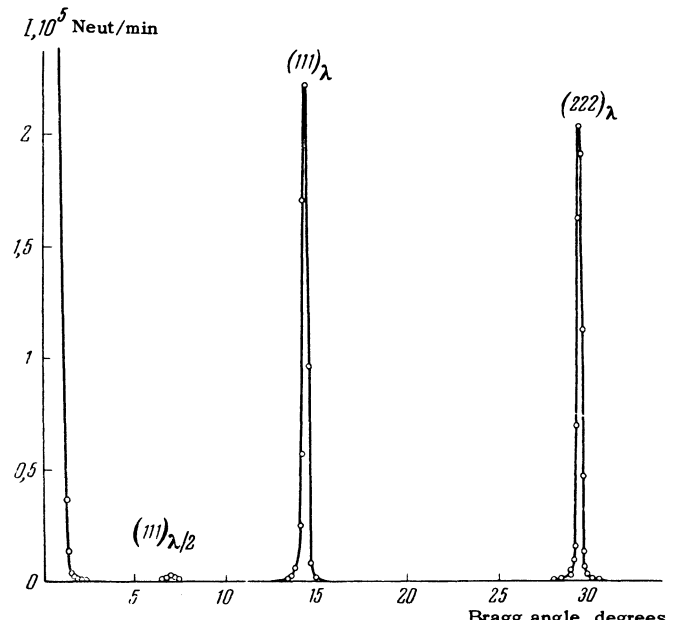


FIG. 6

<sup>2</sup>I. E. Dzyaloshinskiĭ, *J. Exptl. Theoret. Phys. (U.S.S.R.)* **32**, 1547 (1957), *Soviet Phys. JETP* **5**, 1259 (1957).

<sup>3</sup>Alikhanov, Vladimirskiĭ, Nikitin, et al., *Сб. Реакторостроение и теория реакторов (Coll. Reactor Construction and Reactor Theory)*, U.S.S.R. Acad. Sci. Press, 1955, p. 105.

<sup>4</sup>P. Kapitza and P. Cockroft, *Nature* **129**, 224 (1932).

<sup>5</sup>Yu. G. Abov, *Сб. Сессия АН СССР по мирному использованию атомной энергии (Coll. Session of U.S.S.R. Acad. Sci. on Peaceful Use of Atomic Energy)*, М., 1955, p. 294.

<sup>6</sup>R. W. G. Wyckoff, *The Structure of Crystals*, N. Y. Chem. Catalog Co. 1931.

<sup>7</sup>G. E. Bacon, *Neutron Diffraction*, Oxford Univ. Press, 1955; Russ. transl. IIL, 1957.

<sup>8</sup>O. Halpern and M. H. Johnson, *Phys. Rev.* **55**, 898 (1939).

<sup>9</sup>Shull, Strauser, and Wollan, *Phys. Rev.* **83**, 333 (1951).

<sup>10</sup>P. Kapitza, *Proc. Roy. Soc.* **119**, 358 (1928).

<sup>11</sup>H. Bizette, *J. phys. et radium* **12**, 161 (1951).

<sup>1</sup>A. S. Borovik-Romanov and M. P. Orlova, *J. Exptl. Theoret. Phys. (U.S.S.R.)* **31**, 579 (1957), *Soviet Phys. JETP* **4**, 531 (1957).